Journal of Orthopaedic Surgery and Research

RESEARCH

Open Access

Exenatide, a glucagon-like peptide-1 receptor agonist, may negatively impact bone healing in rats: histopathological, biochemical, and in silico findings

Fatih Ugur[1], Ibrahim Yilmaz[2*], Ersin Guner[3], Mehmet Albayrak[4], Recep Taskin[1], Nurtac Sarikas[5], Mehmet Akif Bildirici[6], Ayse Basak Dellalbasi[7] and Candemir Ozcan[7]

Abstract

Background This study evaluates the effects of exenatide (EXE), a glucagon-like peptide-1 (GLP-1) receptor agonist, on bone healing in rats using a single radius cortical defect model and histopathological, biochemical, and in silico methods.

Methods Forty-two male Sprague–Dawley rats, excluding controls, were divided into 7 groups after receiving a standard radius defect. The serum levels of total protein (TP), calcium (Ca^{2+}), phosphorus (P), alkaline phosphatase (ALP), osteocalcin (OC), tumor necrosis factor-alpha (TNF-α), and interleukin-6 (IL-6) in each specimen were measured. Radius samples were examined histopathologically using hematoxylin and eosin (H&E) and Masson's trichrome staining. Molecular docking analyses were used to assess EXE interactions with the GLP-1 receptor and osteogenic transcription factors. Statistical significance was set at $p < 0.05$.

Results Changes in the selected serum markers were observed in the blood samples obtained from the specimens; however, these changes may not have been due to EXE administration. No significant negative effect on bone healing was observed in the groups that received subcutaneous EXE after the bone defect was created. By contrast, it was observed that for the treatment group that received EXE for 7 consecutive days before the bone defect was created on Day 7, bone healing progressed more slowly than in the groups treated with saline. Regarding the binding of EXE to the other target receptors, root mean square deviation (RMSD) values were low, bruised surface area (BSA) was high, and electrostatic interactions were strong, indicating that the ligand (i.e., EXE) binds to the selected receptor surfaces.

Conclusion Although the data obtained from the in vitro analyses in this study were verified using molecular docking, it should be noted that its design is preclinical. Given the widespread clinical use of GLP-1 receptor agonists in the management of type 2 diabetes mellitus (T2DM), our research findings may have translational relevance. Although derived from an experimental animal model, these results suggest that GLP-1 agonists such as EXE can

*Correspondence:
Ibrahim Yilmaz
dryilmazi@yahoo.com

Full list of author information is available at the end of the article

exert additional effects on bone healing and inflammatory processes, thus warranting further studies, including controlled clinical investigations, to elucidate the potential implications for patient care.

Keywords Exenatide, GLP-1 receptor agonist, Inflammatory cytokines, Bone regeneration, Molecular docking

Background

Musculoskeletal disorders rank among the leading contributors to the global disease burden [1]. Individuals can be directly or indirectly predisposed to musculoskeletal disorders by bone defects, which result from regions of impaired healing, tissue loss, or structural gaps due to various causes in bone tissue—the primary support element of the musculoskeletal system [2]. Bone defects can lead to pain, postural instability, gait disturbances, atrophy in the involved muscle groups, reduced mechanical load-bearing capacity, and complications such as chronic osteomyelitis [3]. In addition, bone defects can induce systemic inflammation, as well as muscle and connective tissue degeneration [4].

Notwithstanding the impact of these potential adverse outcomes, conservative, medical, and/or surgical treatment modalities used throughout history to combat these disorders have either shown limited effectiveness or failed to yield satisfactory results [5, 6]. This situation leads to a loss of work capacity and a decrease in patients' quality of life on the one hand, and imposes heavy financial burdens on national healthcare economies on the other [7, 8]. Hence, scientists are intensively researching bone defect repair treatments, with a focus on early diagnosis and intervention for regional lesions.

Animal models of bone defect repair vary considerably, and both unilateral and bilateral approaches are widely used. The unilateral single radius cortical defect model is well established and allows standardized evaluation with low perioperative stress; however, bilateral and multiple critical-sized defect models have also been adopted to improve translational relevance and potentially reduce the number of experimental animals used, which is consistent with the principles of the 3Rs (reduction, replacement, and refinement). Bilateral critical-sized defect models, particularly of long bones such as the femur or tibia, have been shown to provide a robust platform for evaluating regenerative strategies while maximizing the amount of data obtained per animal [9]. Nonetheless, another crucial issue that deserves attention is the investigation and incorporation of new pharmacological agents into future treatments for repairing bone defects.

Exenatide (EXE), a glucagon-like peptide-1 (GLP-1) receptor agonist frequently prescribed for the treatment of type 2 diabetes mellitus (T2DM), has recently gained attention as one of several new pharmacological agents because of its potential effects on bone metabolism. In addition, recent research has highlighted the critical role of cannabinoid receptor signaling in skeletal repair. Cannabinoid receptor 2 (CB2) activation has been shown to modulate the immune environment within the callus, suppressing excessive inflammation and enhancing osteoblast activity, thereby promoting bone healing [10, 11]. These findings highlight the importance of inflammatory immune regulation in bone regeneration and provide a broad mechanistic framework for the investigation of EXE in this study.

Research findings spanning the last decade, although not fully elucidated, suggest that GLP-1 receptors are expressed in osteoblasts and that this pathway may support bone mineralization, osteoblast proliferation, and bone regeneration via anti-inflammatory signaling pathways [12–14]. However, examining the literature revealed that studies report contradictory findings. In addition, there is no high-level, evidence-based study that investigates the effects of EXE on cortical bone healing and sufficiently illuminates inflammatory mechanisms.

This study aims to evaluate the effects of EXE administered to rats using a single radius cortical defect model. For this purpose, total protein (TP), calcium (Ca^{2+}), phosphorus (P), alkaline phosphatase (ALP), tumor necrosis factor-alpha (TNF-α), interleukin-6 (IL-6), and osteocalcin (OC) levels in serum obtained from the blood of living mammalian subjects were tested biochemically. Radius tissue samples were then taken for histopathological evaluation, and the findings were verified using in silico analysis.

Materials and methods

Ethical permissions and general information

Young adult male Sprague–Dawley rats aged 10–12 months and weighing 250–300 g were used as live mammalian subjects in this study. Ethics approval was obtained from the Kastamonu University Experimental Animals Unit to use live mammal subjects in the research (Date: 10.01.2025, approval number: 2025/1). All animal experiments were conducted in accordance with the National Institutes of Health Guide for the Care and Use of Laboratory Animals. Based on welfare considerations, the research subjects were housed under standardized conditions (22 ± 2 °C, 12-h light/dark cycle; free access to food and water; pelleted feed, specially produced for rats and containing 17% protein, 4% fat, and 3% cellulose). Analyses were repeated at least 3 times to detect experimental errors. On the seventh day post operation, all rats were euthanized via a xylazine–ketamine overdose (5 times the anesthetic dose). Intracardiac blood samples were taken at this time. A different set of researchers

administered drugs to the subjects, performed the statistical and in silico analyses, performed the histopathological evaluation, and performed the biochemical evaluation. Each set of researchers was blind to what was administered to which group. In other words, they were blind to the group allocation.

Damage model and experimental study

After the subjects received the relevant infection prophylaxis (intramuscular cefazolin sodium, 20 mg/kg/day) and anesthesia (intraperitoneal xylazine [7 mg/kg] and ketamine [60 mg/kg]), their right forearms (surgical area) were cleaned and disinfected with povidone iodine. Sterile draping was then performed using sterile disposable surgical drapes, and a longitudinal skin incision of approximately 2 cm was made over the mid-diaphysis of the right radius. After incising the skin and subcutaneous tissue, the muscle fascia was reached, and the extensor muscles were gently retracted using blunt dissection to expose the periosteum of the radius. The periosteum was then incised and elevated from the bone surface. On the exposed anterior surface of the radius, a standard unicortical defect 3 mm in diameter was created using a drill bit under constant 0.9% isotonic sodium chloride irrigation, taking care not to penetrate the opposing cortex [15] (Fig. 1).

Afterward, the skin was sutured with 4.0 silk. The surgical wound area was cleaned, and the wound was covered with a dressing.

Group allocation and administration of drugs

A total of 42 rats were randomized into 7 groups (Table 1). Coded labels were affixed to the tails of all rats in each group (n = 6) by the research project administrator. The code was decoded after the experiments and analyses were completed. Except for the project administrator, the researchers were blinded to the group allocation and the drugs administered. EXE treatments were administered subcutaneously once daily (1 μg/kg) [16]. Subjects in the first group received only skin incisions and suturing and were designated as Group 1—the sham group.

Bone healing is a complex process comprising biologically distinct stages [17]. There is an intense inflammatory phase at the onset of the healing process that peaks within the first 72 h following the creation of a bone defect and continues actively for approximately 7 days [18, 19]. Therefore, our study was designed to take this critical early phase of bone healing into account, and the rats were grouped based on a specified timeline (Table 1).

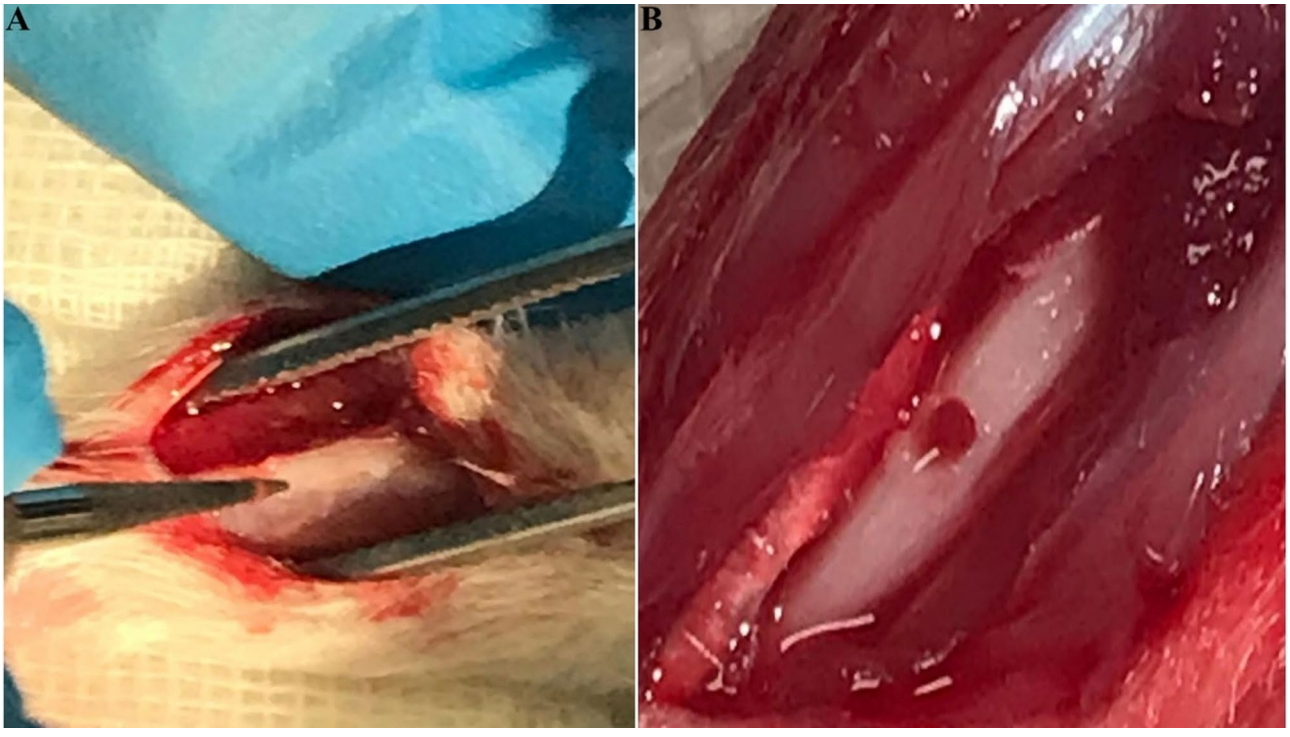

Fig. 1 **A** Intraoperative image of the 3-mm sharp tip of the Dentmotion AAC06 (Lot: DABO1A-35 K/HO1N23DY 0062, China) device approaching the radius. To ensure minimal invasiveness, care was taken to create the bone defect in a controlled manner while preserving tissue integrity. **B** Single cortex defect created in the midline of the radius via surgical procedure, with no obvious hematoma or trauma observed in the surrounding soft tissues. Minimal bleeding within the defect was considered a normal physiological response

Table 1 Experimental groups, bone defect model, and treatment protocols

Group	Bone defect model	Treatment
Group 1 (n = 6)	No bone defect, but there was skin incision and suturing	None
Group 2 (n = 6)	+	None
Group 3 (n = 6)	+	0.9% isotonic sodium chloride for 7 consecutive days post operation
Group 4 (n = 6)	+	EXE for 7 consecutive days before the creation of a bone defect on Day 7
Group 5 (n = 6)	+	EXE for 3 consecutive days post operation
Group 6 (n = 6)	+	EXE for 4–7 days consecutive post operation
Group 7 (n = 6)	+	EXE for 7 consecutive days post operation

Biochemical analysis

Serum prepared from intracardiac blood samples were evaluated for TP, Ca^{2+}, P, ALP, OC, TNF-α, and IL-6 using an enzyme-linked immunosorbent assay (ELISA) and automated biochemistry analyzers. For this purpose, 250 µL blood samples were collected from subjects in all groups under terminal anesthesia at predetermined time intervals. The collected blood was centrifuged at 2,000 × g for 10 min at 25 °C. The sera were aliquoted and stored at – 80 °C until analyzed. TP, Ca^{2+}, inorganic P, and ALP measurements were performed photometrically using a Beckman Coulter AU 5800 (Beckman Coulter Inc., CA, USA) clinical chemistry autoanalyzer and the manufacturer's original brand reagents. As biomarkers, the serum levels of OC, TNF-α, and IL-6 were measured using ELISA kits (Sunredbio, Shanghai, China; cat. nos. 201-11-0765, 201-11-0271, and 201-11-0136, respectively).

Histopathological evaluation

Tissue samples were taken from the control and study groups for histopathological evaluation. Radius samples were fixed with 10% buffered formalin solution for at least 2 weeks, and were then decalcified using a rapid decalcification solution. Subsequently, the samples were washed under running tap water and then subjected to routine paraffinization (incubation in 70%, 80%, 90%, and 100% ethyl alcohol for 1 h, followed by incubation in xylene for 1 h, and finally incubation in paraffin for 1 h). Next, 5 µm sections prepared from the paraffinized tissues were placed on slides and deparaffinized in xylene for 10 min. Hematoxylin and eosin (H&E) staining was then performed. Entellan was dropped on the sections, which were then covered with a coverslip and left to dry. Histopathological changes on prepared slides stained with H&E and Masson's trichrome were observed and evaluated under a light microscope, and photomicrographs were obtained. Changes related to bone healing observed in the samples were scored according to a scoring system developed by Huo et al. [20].

In silico analyses

Evaluation of EXE interaction with potential target proteins

To evaluate the in vivo effects of EXE based on the biochemical and histopathological data obtained, molecular docking was conducted with the rationale that it could provide a mechanistic explanation for the observed effects. The objective was to estimate the binding potential of EXE to the transcription factors/receptors in the signaling pathways involved in bone regeneration and inflammation. For the molecular docking experiments, we obtained crystal structures from the Research Collaboratory for Structural Bioinformatics Protein Data Bank (RCSB PDB). These included the GLP-1 receptor (GLP-1R; PDB ID: 7LLL) [21], the primary target of EXE, as well as other important molecular mediators of the inflammatory response in bone: tumor necrosis factor receptor 1 (TNFR1; PDB ID: 1EXT) [22]; IL-6 receptor (IL-6R; PDB ID: 1P9M) [23]; and the OC receptor, G-protein-coupled receptor family C group 6 member A (GPRC6A), which plays a critical role in osteoblast synthesis.

Molecular docking study

GLP1-R was selected as the target receptor for docking. The GLP-1R crystal structure (PDB ID: 7LLL) was retrieved in PDB format from the RCSB PDB website. The three-dimensional (3D) structure comprises GLP-1R crystallized in complex with its natural agonist, exendin-4, the peptide on which synthetic EXE is based. The P chain containing exendin-4 was extracted from the 7LLL crystal structure via chain separation using the PDB-Tools Web platform. Energy minimization was then performed on the isolated exendin-4, which was saved in PDB format for use as the ligand in all docking experiments conducted in this research. The active residues of exendin-4 were subsequently identified using ChimeraX (version 1.10).

Molecular docking experiment with GLP-1R

The R chain containing GLP-1R protein was separated from the 7LLL crystal structure using the PDB-Tools Web platform. All water molecules were removed, and polar hydrogens were added. The web-based High Ambiguity Driven DOCKing (HADDOCK) server (version 2.4) was used for protein–protein docking. The active residues of the computationally prepared GLP-1R were scanned and extracted using ChimeraX 1.10, and docking was performed.

Molecular docking study with TNFR1

The A chain containing the TNFR1 protein was separated from the 1EXT crystal structure using the PDB-Tools Web platform. All water molecules were removed, and polar hydrogens were added. The web-based HADDOCK 2.4 server was used for protein–protein docking. The active residues of the prepared TNFR1 were scanned and extracted using ChimeraX 1.10, and docking was performed.

Molecular docking study with IL-6R

The A chain containing the IL-6R protein was cleaved from the 1P9M crystal structure using the PDB-Tools Web platform. All water molecules were removed, and polar hydrogens were added. The web-based HADDOCK 2.4 server was used for protein–protein docking. The active residues of the prepared IL-6R were scanned and extracted using ChimeraX 1.10, and the docking process was performed.

Molecular docking study with GPRC6A

No crystallized 3D structure (X-ray or cryo-EM) is available for GPRC6A in the RCSB PDB. Hence, its protein sequence (UniProt ID: Q5T6X5) was modeled using the AlphaFold Protein Structure Database. The web-based HADDOCK 2.4 server was used for protein–protein docking. Active residues of the prepared GPRC6A were scanned and extracted using ChimeraX 1.10, and docking was performed.

Molecular docking study with RUNX2

The D chain containing the runt-related transcription factor 2 (RUNX2) protein was isolated from the crystal structure with PDB ID GVGE using PDB-Tools Web. All water molecules were removed, and polar hydrogens were added. The web-based HADDOCK 2.4 server was used for protein–protein docking. The active residues of the prepared RUNX2 chain were scanned and extracted using ChimeraX 1.10, and the docking process was performed.

Statistical analyses

The Minitab (version 22) program was used for the statistical analysis of the obtained data. Group differences were detected by an analysis of variance (ANOVA), and Tukey's honest significance (HSD) test was applied to determine which groups' means were different. Tukey's HSD test is a post hoc test performed to group the distribution data following descriptive analysis, and thus evaluate the differences between group means. The strength of the relationship between the tested target markers Ca^{2+}, P, ALP, TNF-α, IL-6, and OC and their relationships with each other were evaluated using the Pearson correlation coefficient (r). The data were assessed at a 95% confidence interval (CI), and an alpha of < 0.05 was considered statistically significant.

Results

Biochemical findings

Compared to the control group (Group 1), serum Ca^{2+} levels decreased in Groups 3, 4, and 7 and increased in all the other groups. However, because the difference in serum Ca^{2+} levels between the groups was statistically insignificant (p >0.05), this observation was not taken into consideration. Compared to the control group, serum TP levels decreased in Group 4 and increased in all the other groups ($p < 0.05$). The serum levels of P decreased in Groups 2, 5, 6, and 7 compared to the control group and increased in all the other groups ($p < 0.05$). Serum ALP levels decreased in all groups ($p < 0.05$). Serum TNF-α levels increased in Groups 3 and 6 compared to Group 1 and decreased in all the other groups ($p < 0.05$). Compared to Group 1, the serum levels of IL-6 and OC increased ($p < 0.05$) in all the other groups (Tables 2 and 3).

There was a strong positive correlation between the serum levels of Ca^{2+} and TP (r = 0.710; $p < 0.05$), a moderately strong negative correlation between P and TP levels (r = – 0581; $p < 0.05$), and a slightly above-moderate negative correlation between P and Ca^{2+} levels (r = – 0.643; $p < 0.05$). Other correlations were not statistically significant (p >0.05) and were therefore excluded from our analysis (Fig. 2).

Histopathological findings

No significant negative effect on bone healing was observed in the groups that received subcutaneous EXE after the bone defect was created. However, it was observed that when the bone defect was induced in a subject already receiving EXE, bone healing progressed more slowly than in subjects in other treatment groups (i.e., EXE post-surgery groups and the post-surgery saline group [Group 4]). Histological evaluation of bone healing based on Huo scoring among the experimental groups is summarized and presented in Fig. 3.

Because the regions representing the bone defect site were not visible in the sections stained with Masson's trichrome for technical reasons, the Masson's trichrome stained slide representing Huo score 7 was excluded from our evaluation. The remaining slides are presented demonstratively in Fig. 4.

In silico findings

Data from the outputs of the analyses using the ChimeraX 1.10 molecular modeling program were used to generate images of the 3D protein–ligand complex. In these images, the receptor and ligand protein are superimposed

Table 2 Data from analysis of variance (ANOVA) with 95% CI comparing the control and EXE groups

	Source	DF	Adj SS	Adj MS	F-Value	P-value
TP	Group	6	1.058	0.17635	3.48	0.08*
	Error	35	1.773	0.05067		
	Total	41	2.831			
Ca^{2+}	Group	6	1.233	0.2056	1.91	0.106
	Error	35	3.760	0.1074		
	Total	41	4.993			
P	Group	6	44.44	7.406	4.32	0.002*
	Error	35	60.07	1.716		
	Total	41	104.51			
ALP	Group	6	81,241	13,540	13.44	0.000*
	Error	35	35,252	1007		
	Total	41	116,493			
TNF-α	Group	6	34,118	5686	2.93	0.020*
	Error	35	67,855	1939		
	Total	41	101,973			
IL-6	Group	6	4220	703.3	2.49	0.041*
	Error	35	9881	282.3		
	Total	41	14,101			
OC	Group	6	29.17	4.8613	5.73	0.000*
	Error	35	29.72	0.8490		
	Total	41	58.88			

*One-way ANOVA, $p < 0.05$

DF: degrees of freedom; Adj SS: adjusted sum of square; MS: mean square

Table 3 Data obtained from Tukey's honest significance (HSD) test

	TP	Ca^{2+}	P	ALP	TNF-α	IL-6	OC
Group 1	5.95 ± 0.06 AB	10.25 ± 0.38ns	8.30 ± 0.11ABC	300.5 ± 1.64 A	177.33 ± 3.31AB	80.03 ± 7.42B	3.44 ± 0.11C
Group 2	6.35 ± 0.06 A	10.55 ± 0.54ns	6.9 ± 0.55ABC	261.0 ± 38.34AB	153.92 ± 16.86AB	85.98 ± 4.85AB	4.60 ± 0.61ABC
Group 3	6.27 ± 0.44AB	10.17 ± 0.68ns	8.93 ± 3.08AB	190.7 ± 28.97C	227.58 ± 85.2A	82.20 ± 5.8AB	4.01 ± 0.79BC
Group 4	5.90 ± 0.17B	10.05 ± 0.12ns	9.10 ± 0.88A	294.8 ± 37.31A	174.48 ± 53.8AB	110.69 ± 27.9A	5.32 ± 0.89AB
Group 5	6.02 ± 0.18AB	10.28 ± 0.13ns	6.65 ± 0.84BC	212.7 ± 26.64BC	125.82 ± 8.8B	94.17 ± 22.02AB	5.98 ± 1.74A
Group 6	6.23 ± 0.18AB	10.47 ± 0.24ns	6.35 ± 0.33C	196.0 ± 48.48C	182.43 ± 36.3AB	95.46 ± 21.38AB	5.44 ± 0.4AB
Group 7	6.08 ± 0.25AB	10.10 ± 0.23ns	7.68 ± 0.81ABC	202.8 ± 23.83C	176.9 6 ± 41.62AB	82.80 ± 11.98AB	4.24 ± 0.97BC

ns: statistically nonsignificant and the significance level between groups decreases from A to C

onto the protein–protein binding region in all docking results (Fig. 5).

Based on the evaluation of the binding properties of the molecules, the results of EXE to the target receptors are presented in Table 4.

Examining the binding of EXE with other target receptors, the root mean square deviation (RMSD) values were low, bruised surface area (BSA) was high, and electrostatic interactions were strong. This indicates that the ligand binds to the selected receptor surfaces.

Discussion

Current strategies for accelerating fracture healing include both pharmacological and physical approaches. Systematic reviews have demonstrated that pharmacological agents can positively influence fracture healing, and that randomized controlled trials provide growing evidence for the clinical potential of several pharmacological agents [24]. Similarly, low-intensity pulsed ultrasound (LIPUS) has been shown to stimulate osteogenesis and support fracture healing in vitro and in animal models, although clinical evidence remains limited [25]. Recently, pharmacological interventions such as pulsed electromagnetic field therapy have been reported to facilitate osteogenic differentiation and fracture healing via modulation of key molecular signaling pathways, including osteogenesis-related cascades [26]. Also, adjunctive strategies such as low-level laser therapy have been reported to enhance osteoblast activity, angiogenesis, and fracture healing, highlighting the complexity of bone regeneration mechanisms [27].

In addition, it has been reported that mechanical interventions, such as intermittent pneumatic compression, enhance both bone and soft-tissue healing, although stronger evidence from human studies is still required [28].

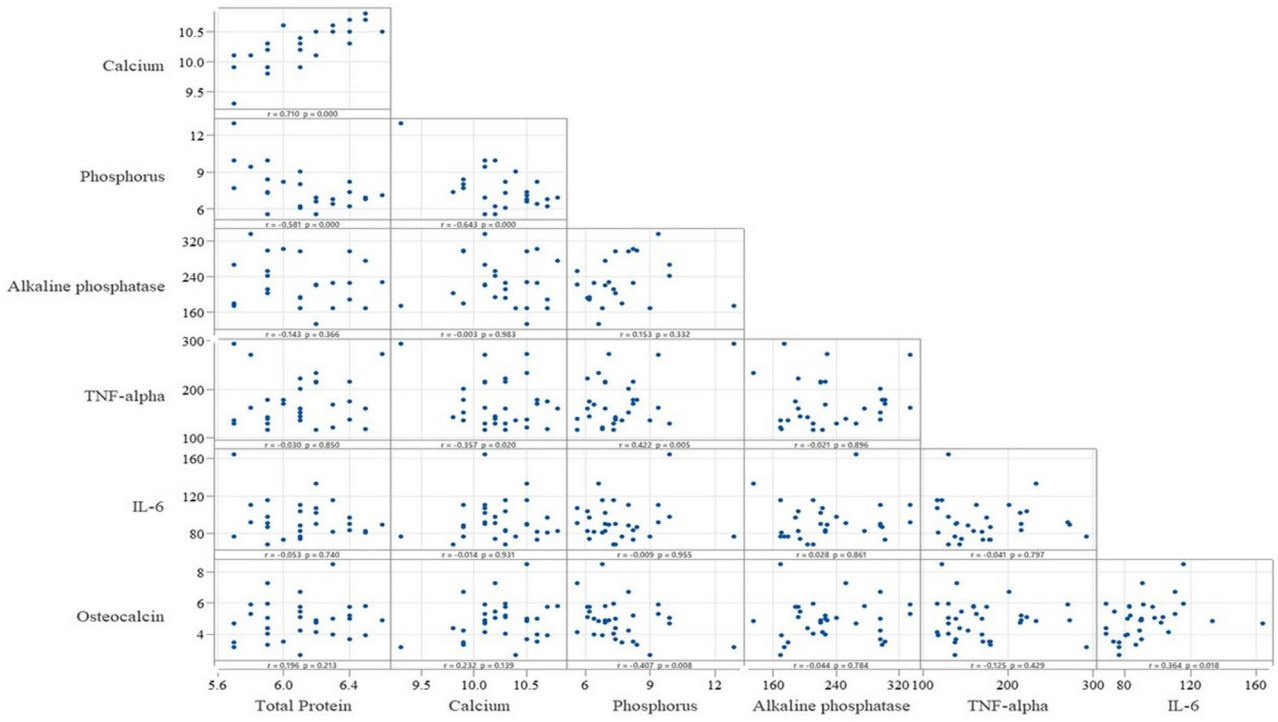

Fig. 2 Matrix plot of Ca^{2+}, P, ALP, TNF-α, IL-6, and OC serum levels. ρ: pairwise Pearson correlation

The literature also suggests that EXE may promote bone regeneration by regulating inflammatory responses and promoting osteogenic activity. Interestingly, similar mechanisms have been identified in studies on cannabinoid receptor signaling—particularly studies on CB2, which reduces proinflammatory cytokine release and stimulates osteoblast differentiation in fracture healing [10, 11]. This suggests that GLP-1R activation and cannabinoid receptor pathways may converge in common immune–bone signaling networks, highlighting a promising translational link between metabolic and cannabinoid-based interventions in skeletal repair.

Our study contributes to this growing body of evidence by providing histopathological and biochemical insights into the effects of EXE, as a GLP-1R agonist, in bone healing and validating our observations using in silico methods.

Ji et al. [29] made a novel pharmacological contribution to fracture healing research in their study evaluating the histopathological and biochemical effects of EXE, as a GLP-1R agonist, in a single radius cortical defect model. Considering that EXE exerts important metabolic regulatory effects, its potential relevance is particularly notable in fracture patients at risk of impaired healing due to hyperglycemia [29].

Recent findings further emphasize the significance of pharmacological and molecular targets in bone regeneration. For example, Jintiange has been reported to accelerate fracture healing in osteoporotic rat models [30], miR-1271-5p has been reported to promote healing in pilon fractures by regulating apoptosis and chondrocyte proliferation [31], and lncRNA CASC11 has been reported to delay fracture healing by sponging miR-150-3p [32]. Similarly, LINC00339 has been implicated in the modulation of mesenchymal stem cell osteogenic differentiation and delayed fracture healing [33].

These studies highlight new perspectives for advancing fracture healing research, presented by the integration of pharmacological interventions and molecular biology. However, when sequential searches were made in electronic databases using relevant keywords, we observed that the data obtained were different and contradictory [34–49]. For example, one study reported that GLP-1R agonists (GLP-1RAs) may have beneficial effects on bone [34]. In contrast, another study reported that exendin-4 reduced serum levels of a bone resorption marker, C-terminal cross-linked telopeptides of type I collagen, but increased the osteoprotegerin/receptor activator of nuclear factor-κB (NF- κB) ligand ratio and elevated OC, RUNX2, and ALP expression; and thus, bone resorption was not inhibited [35]. Similarly, another study found that when rat bone marrow stromal cells (BMSCs) were treated with exendin-4, mRNA expression levels of Runx2, ALP, and collagen-α1 increased, indicating that exendin-4 exerts an anabolic effect on bone by facilitating osteoblastogenesis while suppressing adipogenesis during BMSC lineage differentiation in ovariectomized rats [36]. In addition, EXE (the synthetic analog of exendin-4)

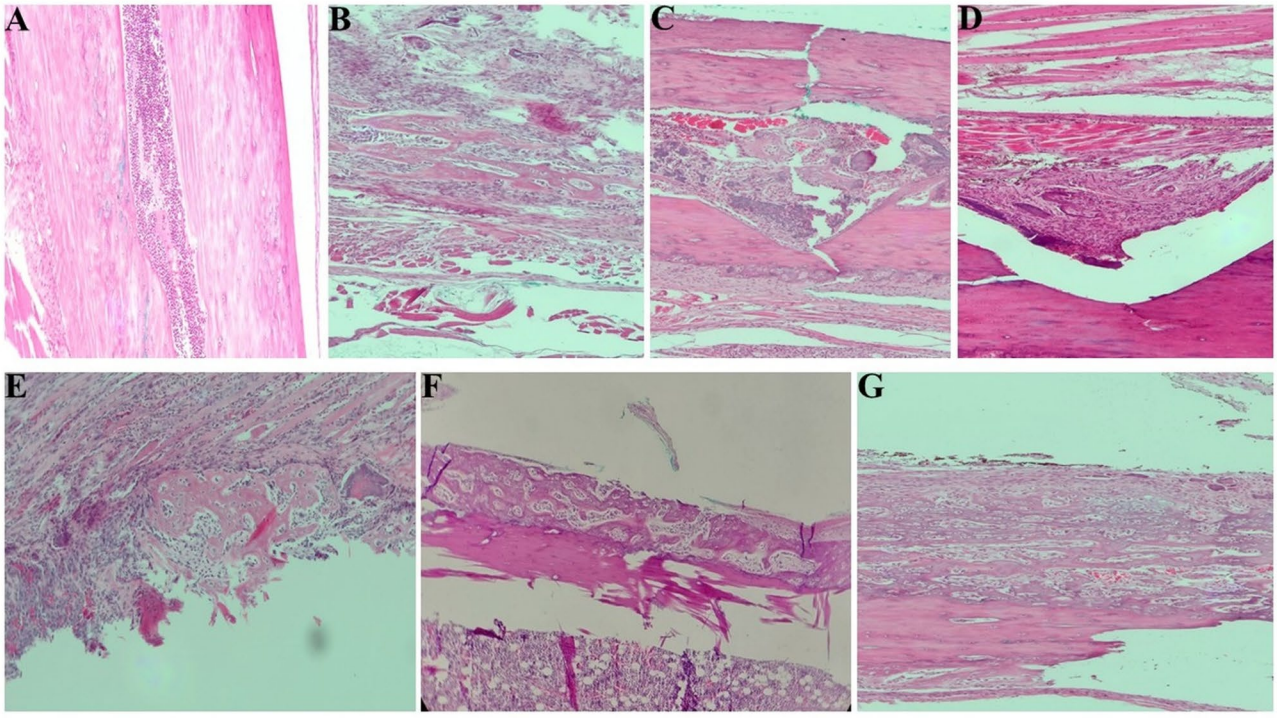

Fig. 3 Images captured with a light microscope at 100× magnification after H&E staining. **A**: *Group* 1 (control group – no bone defect): No bone defects were created or observed in the experimental animals in this group. The cortical bone and medullary spaces appeared structurally regular and intact. Because no experimental injury was induced, Huo histological scoring could not be applied. **B**: *Group 2* (fracture union through immature bone formation): Predominantly osteoid-like structures were present, accompanied by intense osteoblastic activity. The Huo score for this group was 9. **C**: *Group 3* (mixed cartilage and osteoid tissue): A nearly equal distribution of cartilage and osteoid tissue was observed. The Huo score for this group was 7. **D**: *Group 4* (fibrous tissue): Only fibrous tissue was detected at the site of the bone defect. The Huo score was 1. **E**: *Group 5* (predominantly osteoid tissue with limited cartilage): Dense osteoid tissue was observed with minimal cartilage presence. The Huo score for this group was 8. **F**: *Group 6* (high osteoblastic activity with minimal fibrous tissue): Marked osteoblastic activity was evident, while fibrous tissue was nearly absent. This group received a Huo score of 8. **G**: *Group 7* (predominantly immature bone with minimal cartilage): Immature bone tissue was the dominant component, along with a small amount of cartilage. The Huo score for this group was 8.

has been reported to improve bone quality in a genetically inherited T2DM mouse model [37].

Overall, experimental studies have shown that GLP-1RAs exert significant positive skeletal effects on bone quality and bone strength; however, the mechanisms of action may differ among the various GLP-1RAs, and clinical studies supporting their bone-protective effects are currently lacking [38]. The possibility that GLP-1RAs may improve blood flow to bone has attracted considerable attention and suggests that GLP-1 antidiabetic therapy may benefit the increasing number of elderly T2DM patients at a substantial risk of osteoporosis and fractures [38].

Eminoy et al. [39] reported a significant decrease in bone mineral density, trabecular number, trabecular thickness, and trabecular area in ovariectomized rats, as well as a significant increase in trabecular separation and plasma TNF-α and IL-6 levels. They reported that all these adverse effects were reversed with EXE treatment, which exhibited a significant protective effect on trabecular bone microarchitecture [39]. Mansur et al. [40] used male, high-fat, diabetic mice in their study to evaluate the effects of EXE treatment on tissue-bone mechanical properties and composition parameters. They administered EXE intraperitoneally to the subjects at a dose of 25 nmol/kg twice daily for 52 days. They reported significant improvements in bone mechanical properties at the organ and tissue levels, with observable changes in both cortical microarchitecture and bone composition parameters, in the EXE-treated group compared to the control group [40].

In addition to in vitro and/or in vivo experimental preclinical studies using living mammalian subjects, there have also been clinical studies, with positive outcomes indicating that EXE can facilitate the healing of bone fractures. In a placebo-controlled study evaluating patients treated with GLP-1RAs, EXE use was associated with the lowest risk of fracture compared to other GLP-1RAs [36]. The findings of another placebo-controlled clinical trial (NCT01648582) indicate that GLP-1RAs may reduce the risk of bone fragility in patients with T2DM, as they increase bone mineral density in many areas of the

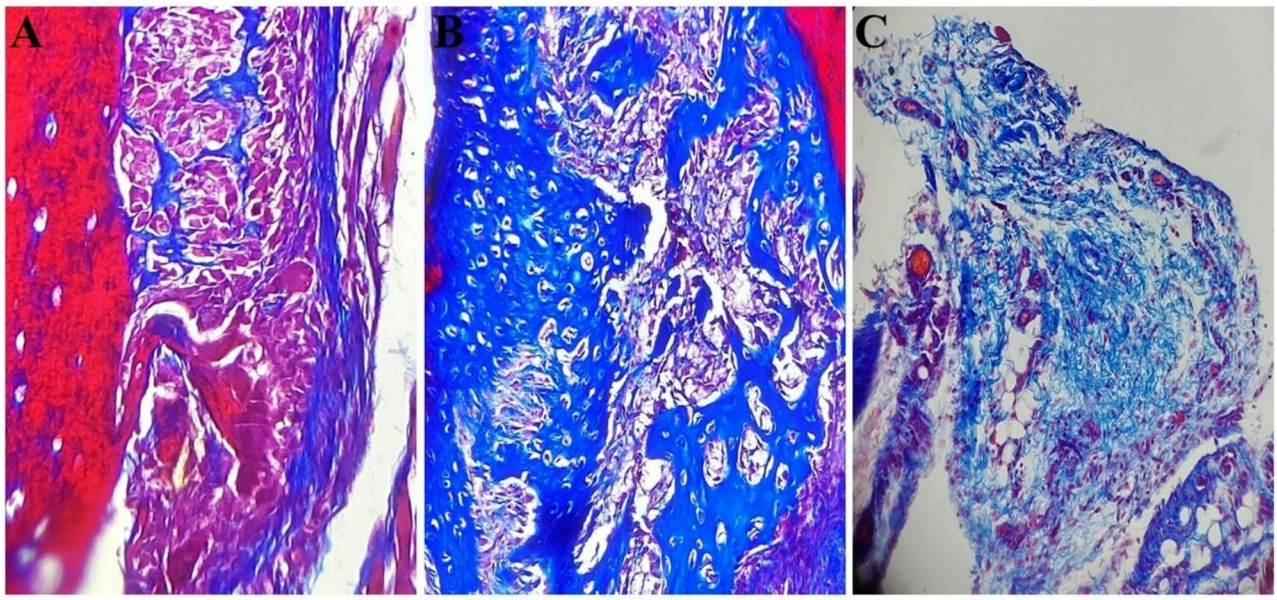

Fig. 4 Masson's trichrome staining of preparations at ×200 magnification. **A** Predominantly immature bone is visible, and a small amount of cartilage is observed; Huo score 8. **B** Only immature bone is visible; no cartilage is observed; Huo score 9. **C** Fibrous tissue is visible, but no immature bone and/or cartilage is observed at the fracture site; Huo score 1

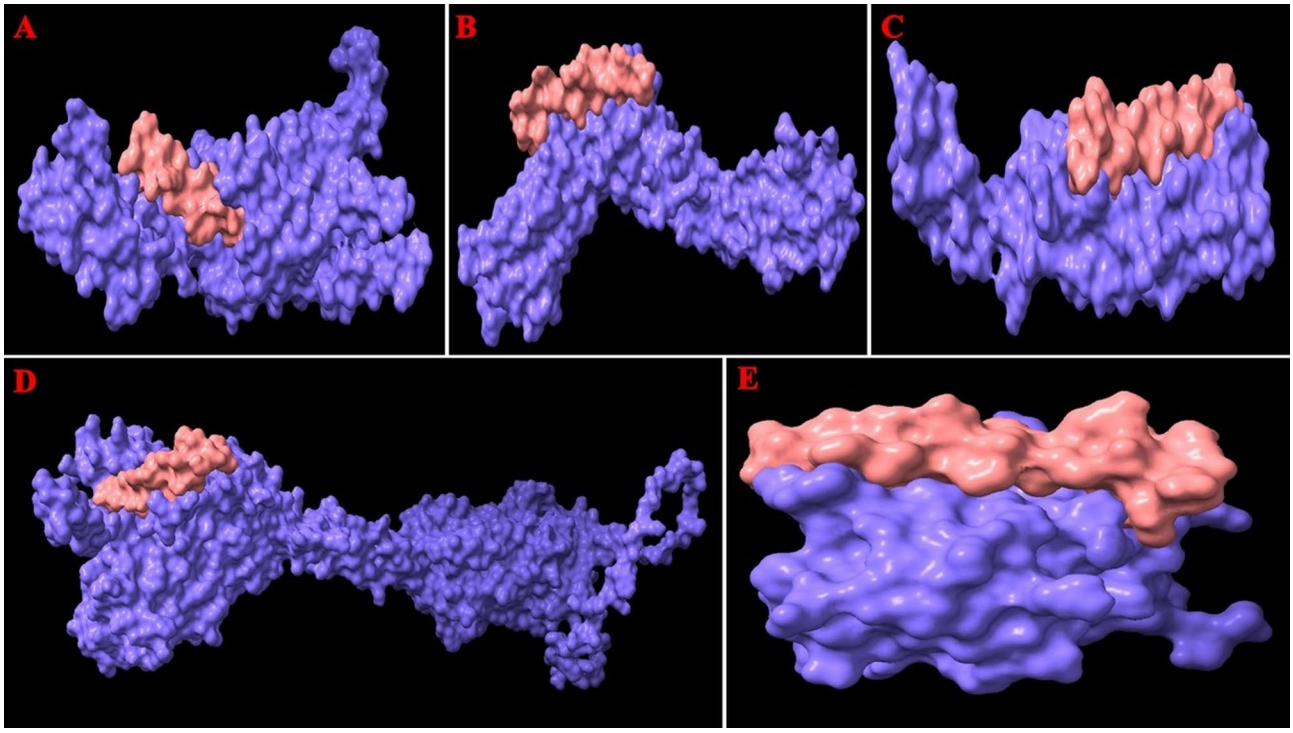

Fig. 5 Receptor-EXE interactions analyzed using the ChimeraX 1.10 molecular modeling software. **A** GLP-1R-EXE, **B** IL-6R-EXE, **C** TNFR1-EXE, **D** GPRC6A-EXE, **E** RUNX2-EXE. Pink indicates EXE, and purple indicates the receptor

body after treatment [41]. Another study reported that GLP-1RAs, including EXE, may heal bone fractures in patients with T2DM [42]. Akyay et al. [43] reported that osteoprotegerin levels increased and resorption markers, such as the receptor activator of NF- κB (RANK)/receptor activator of NF- κB ligand (RANKL) ratio, decreased with EXE treatment. They concluded that GLP-1RAs exhibit a potential fracture-protection effect [44].

Table 4 Docking results: EXE to target receptors

Receptor	Ligand	HADDOCK score (kcal/mol)	RMSD	BSA	Z-score
GLP-1R	EXE	− 156.6	1.1	2503.6	− 2.5
TNFR1	EXE	− 97.0	2.0	1698.6	− 0.9
IL-6R	EXE	− 105.3	0.3	1574.3	− 2.2
GPRC6A	EXE	− 98.2	0.2	1714.1	− 1.9
RUNX2	EXE	− 89.6	0.5	1729.6	− 2.3

BSA: bruised surface area; RMSD: root mean square deviation

Contrary to the preceding definitive reports, there are studies in the literature with findings indicating that traditional antidiabetic drugs may have negative or positive effects on the risk of bone fractures. However, the relationship between GLP-1RAs and bone fracture risk has not yet been established. Notably, however, EXE treatment has been associated with an increased risk of new bone fractures [45]. Although preliminary, there is a study in the literature reporting that GLP-1RA use does not alter the risk of bone fractures [46]. Furthermore, a post hoc analysis found a study [42] that reported an absence of evidence of EXE treatment having any impact on bone fractures, and a letter [47] suggesting that this issue should be discussed.

Responding to these confusing and contradictory findings in the literature, our study was conducted to verify the effects of the pharmacological agent EXE in silico after evaluating it in vitro following its administration to rats in which a bone defect was surgically created.

The relationship between serum protein levels and bone health is complex. Serum TP levels have been reported to support cellular proliferation and extracellular matrix synthesis in bone fracture healing [48]. In this study, serum TP levels decreased in Group 4 and increased in the other groups compared to the control group.

Ca^{2+} has been established as the fundamental building block of callus mineralization. Normal serum Ca^{2+} levels ensure strong and adequate mineralization at fracture sites [49], while inadequate Ca^{2+} intake leads to post-traumatic bone loss and increased parathormone and osteoclast activity, which impair overall bone health [50]. Bone growth and metabolism are also regulated by trace elements, such as Ca^{2+} and P. It has been hypothesized that both trace element deficiencies and excesses may be risk factors for the development of bone diseases, such as osteoporosis [51].

In our study, Ca^{2+} levels decreased in Groups 3, 4, and 7 and increased in Groups 2, 5, and 6 compared to the control group (Group 1). However, because this difference in Ca^{2+} levels between groups was found to be statistically insignificant (p >0.05), it cannot be considered as evidence of the effect of EXE administration on Ca^{2+} levels. Furthermore, P levels decreased in Groups 2, 5, 6, and 7 but increased in Groups 3 and 4 compared to the control group; the largest increase, at 9.64%, was observed in Group 4.

Although its precise role is not fully elucidated, ALP—which is thought to play a role in bone mineralization—is the most widely known biochemical marker of osteoblast activity [50]. The literature also includes studies suggesting that both TNF-α and IL-6 may promote osteogenic differentiation by stimulating ALP [52], and that serum ALP levels increase in the early post-surgery phase [53]. One study found a negative correlation between total serum ALP levels and lumbar body mass index in young adults, proposing that total ALP and bone-specific ALP are byproducts of bone remodeling and can be measured in serum as indicators of the rate of bone turnover [54]. Another study reported that ALP levels began to slowly increase 2 weeks after surgery [55]. In our study, ALP levels were found to be reduced in all groups compared to the control group ($p < 0.05$), which may be because the serum ALP values were measured 7 days after the trauma.

TNF-α may have different effects on different signaling pathways in bone pathophysiology. Depending on the cell type and the receptor activated, it can induce apoptotic or survival signals. Furthermore, recent evidence suggests that signaling in osteoclasts generally has a proliferative effect, while signaling in osteoblasts and osteocytes has an inhibitory effect [56]. If the TNF-R1 and TNF-R2 signaling pathways are activated by TNF-α, MAPK phosphorylation and NF-κB pathways can be activated in osteoclasts, osteoblasts, and osteocytes [56, 57]. This may cause delays in both the early inflammation and late healing phases due to TNF-αR deficiency [58]. Interestingly, in our study, TNF-α levels were found to increase by 28.33% and 2.88% in Groups 3 and 6, respectively, compared to the control group ($p < 0.05$), but decreased in all the other groups ($p < 0.05$).

TNF-α also induces transcriptional activation of genes that indirectly promote bone resorption in osteoblasts, such as the IL-6 and NF-κB genes [59]. A review of recent studies in the literature that used living mammalian subjects suggests that neutrophil-mediated IL-6 signaling is essential for physiological bone turnover and fracture healing, while revealing that the role of IL-6 signaling in impaired healing under conditions of excessive inflammation remains to be determined [60]. In contrast, due to its key role in both systemic post-traumatic inflammation and fracture healing, the pleiotropic cytokine IL-6 has been reported to play a role in the pathomechanisms of impaired fracture healing caused by trauma [61]. Furthermore, selective inhibition of IL-6 trans-signaling has been confirmed by accelerated cartilage-to-bone transformation, strengthened bone bridging of the fracture gap, and improved mechanical callus properties

[61]. Although global IL-6 inhibition has been reported to significantly improve post-traumatic fracture healing outcomes, it has also been highlighted that while selective inhibition of IL-6 trans-signaling does not impact impaired fracture healing, it may have therapeutic potential for treating fracture healing complications [61].

Pesic et al. [62] found that serum TNF-α levels did not show a statistically significant change in the early phase of fracture healing in elderly patients with femur fractures, while IL-6 levels showed a statistically significant increase on the first day after the intervention. In our study, serum IL-6 levels increased in all groups compared to the control group, with the highest increase being in Group 4, at 38.31%.

There are also studies in the literature suggesting that OC plays no role in exercise-induced bone formation [63, 64]. It has also been reported that the carboxylated form of OC—which is secreted by osteoblasts and is the most abundant non-collagenous protein in bone—supports bone mineralization and increases bone strength [65]. OC levels have been reported to increase following a fracture and, in most cases, remain at slightly higher levels throughout the healing process compared to the time of trauma [53]. Similarly, in our study, serum OC levels were observed to increase in all groups compared to Group 1. This increase was greatest in Group 5 (73.84%), followed by Group 6 (58.14%) and Group 4 (54.65%). However, it cannot be concluded that the increase in serum OC levels observed in these groups was due to EXE administration.

In summary, except for serum Ca^{2+} levels, the intergroup comparisons of all serum markers evaluated in this study were found to be statistically significant ($p < 0.05$). Furthermore, the study revealed a strong positive correlation between the serum levels of Ca^{2+} and TP, and a moderately strong negative correlation between the serum levels of P and TP. A slightly greater-than-moderate negative correlation was found between the serum levels of P and Ca^{2+}, along with a weak negative correlation between the serum levels of TNF-α and Ca^{2+}, and a weak positive correlation between the serum levels of TNF-α and P. A weak negative correlation was found between the serum levels of IL-6 and Ca^{2+} and those of IL-6 and P, with a weak positive correlation between the serum levels of IL-6 and ALP. In addition, a weak positive correlation was found between the serum levels of OC and IL-6. Based on the histopathological evaluation, the lowest Huo scores were in Group 4 (Huo score = 1), Group 3 (Huo score = 7), followed by Groups 5, 6, and 7 (Huo score = 8). The highest Huo score was in Group 2 (Huo score = 9).

In our study, bone regeneration was evaluated using histopathological methods, which offer valuable qualitative insights into tissue architecture and healing. However, histomorphometric analysis is widely considered the gold standard for quantitatively assessing new bone formation and bone remodeling. Chatzipetros et al. [66] demonstrated the strength of histomorphometric approaches in providing precise measurements of bone volume, trabecular thickness, and other microstructural parameters that cannot be captured by qualitative assessment alone. Although our findings support the regenerative potential observed, the lack of histomorphometric data limits the quantitative interpretation of bone healing in our model. Future studies incorporating histomorphometry would provide a more comprehensive evaluation of the extent and quality of bone regeneration.

When the possible EXE interactions with selected proteins involved in inflammation and bone metabolism were evaluated using the HADDOCK-based protein–protein docking method, the strongest interaction was shown to be with GLP-1R (HADDOCK score = – 156.6 kcal/mol; BSA: 2503.6 $Å^2$; Z-score: – 2.5). These findings confirm the high-affinity binding of EXE to its known pharmacological target and support the validity of the docking protocol. Remarkably, EXE also showed high-affinity binding with IL-6R (HADDOCK score = – 105.3 kcal/mol; RMSD: 0.3 Å; Z-score: – 2.2). This suggests the possibility of direct interaction with inflammatory signaling pathways. Considering that IL-6 plays a dual role in both bone healing and systemic inflammation, this molecular interaction may explain the increase in serum IL-6 levels, especially in the group that received EXE before the defect was created (Group 4). The excessive IL-6 response observed in this group may have created an imbalance in inflammation regulation, resulting in delayed healing, consistent with the histopathologically low Huo score.

Similarly, significant binding was observed with GPRC6A, the known OC receptor (HADDOCK score = – 98.2 kcal/mol; RMSD: 0.2 Å; Z-score: – 1.9). This result supports a possible interaction with osteoblast-related signaling pathways. This molecular binding also coincides with an increase in serum OC levels in the EXE groups. Furthermore, this suggests that EXE may modulate bone formation via GPRC6A, in addition to GLP-1R. Binding with TNFR1 was found to be weaker than with other receptors (HADDOCK score = – 97 kcal/mol; RMSD: 2.0 Å; Z-score: – 0.9). This suggests that EXE may not directly impact TNF-α, but may indirectly modulate its pathways. This is consistent with the fact that the serum TNF-α levels varied between the groups in the study. In addition, in the docking study conducted with the RUNX2 transcription factor—which plays a key role in osteoblast differentiation—it was determined that EXE exhibited moderate binding (HADDOCK score = – 89.6 kcal/mol; RMSD: 0.5 Å). This finding highlights the

possibility that EXE may directly affect osteogenic gene expression at the transcriptional level.

Limitations

The sensitivity of human tissues differs from that of animal tissues [67]. Therefore, data obtained from living mammalian subjects may differ from data obtained from humans [68, 69]. Although serum Ca^{2+}, P, ALP, OC, TNF-α, and IL-6 provide systemic information regarding bone metabolism and the inflammatory process, these parameters are not sufficiently bone-specific to fully reflect differences in local healing. Highly specific biomarkers such as bone-specific ALP (BSALP) or tartrate-resistant acid phosphatase 5b (TRAP5b), which are directly related to osteoblast and osteoclast activity, could provide a more accurate evaluation of the remodeling stage. Future research incorporating bone-specific biomarkers will contribute to a more detailed understanding of bone healing dynamics. We employed a single radius cortical defect model, which is reproducible and avoids the need for internal fixation; however, as a non-load-bearing bone, its translational relevance is lower than that of femoral or tibial models. In addition, we focused on histopathological, biochemical, and in silico evaluations without including micro-computed tomography or biomechanical analyses, which limits quantitative assessment of bone regeneration. Furthermore, evaluations were performed only on Day 7, thus capturing early inflammatory and fibrocartilaginous phases and not complete bone healing; longer follow-up periods are required for a comprehensive assessment. An interesting finding is that EXE pretreatment appeared to delay bone healing, while posttreatment had more favorable effects. Although the precise mechanisms were not investigated, previous studies suggest that GLP-1R agonists may modulate NF-κB, MAPK, and oxidative stress pathways, which may underpin these observations. Further mechanistic analyses, including immunohistochemistry and molecular pathway studies, are needed to clarify this postulation. In addition, this study employed in silico methods. However, the docking analyses in this study were performed only on static crystal structures and were not supported by molecular dynamics simulations. Therefore, the results should be interpreted strictly in the context of generating biological hypotheses, rather than for definitive mechanistic verification. Notably, however, to overcome the limitations inherent in in silico approaches, the biological validity of the in silico data was enhanced by data obtained from in vitro laboratory analyses.

Conclusion

When all the findings are evaluated together, the in silico docking data, in alignment with the biochemical and histopathological findings, offer a possible molecular mechanism for the versatile positive or negative effects of EXE on bone healing. These molecular data suggest that GLP-1R agonists may impact not only glycemic control but may also act on inflammatory and osteogenic pathways. Thus, clinicians must carefully consider possible precautions against potential negative impact on bone fractures in T2DM cases and cases in which EXE is already being administered.

Abbreviations

ALP	Alkaline phosphatase
BSA	Bruised surface area
Ca^{2+}	Calcium
CB2	Cannabinoid receptor 2
EXE	Exenatide
GLP-1	Glucagon-like peptide-1
GLP-1RA	Glucagon-like peptide-1 receptor agonist
GPRC6A	G protein-coupled receptor family C Group 6 member A
IL	Interleukin
OC	Osteocalcin
P	Phosphorus
RANKL	Receptor activator of nuclear factor-κB ligand
RMSD	Root mean square deviation
RUNX2	Runt-related transcription factor 2
T2DM	Type 2 diabetes mellitus
TNF-α	Tumor necrosis factor-alpha
TP	Total protein

Acknowledgements

None.

Author contributions

FU and IY conceived and designed the experiments. FU, IY, and EG were responsible for methodology, formal analysis, and writing the original draft. IY and EG calculated the drug doses to be administered to the subjects and interpreted them by performing in silico analyses. FU, IY, and EG performed the statistical analyses of the data. NS provided and interpreted the histopathological evaluation and scoring of the obtained tissue samples. MAB performed and interpreted the ELISA study on the serum obtained from the blood of the subjects. FU, MA, and RT were responsible for conceptualization and funding acquisition. FU, RT, ABD, and CO provided care for the subjects, performed drug administration, and developed the surgical experimental animal model. FU, IY, EG, MA, NS, and MAB were responsible for validation and the writing, review, and editing of the research manuscript. All authors agreed to be equally accountable for all aspects of the research. All authors approved the final manuscript.

Funding

This research did not receive any funding.

Data availability

The datasets used or analyzed in this study are available upon reasonable request from the corresponding author.

Declarations

Ethics approval

Ethics approval to use live mammal subjects in the research was obtained from the Kastamonu University Experimental Animals Unit (Date: 10.01.2025, approval number: 2025/1).

Consent for publication

Not applicable.

Competing interests

The authors declare no competing interests.

Author details

[1]Department of Orthopedics and Traumatology, Kastamonu University School of Medicine, 37200 Kastamonu, Turkey

[2]Unit of Pharmacovigilance, Republic of Turkey, Ministry of Health, Dr. Ismail Fehmi Cumalioglu City Hospital, 59020 Tekirdag, Turkey
[3]Department of Pharmacy, Republic of Turkey, Ministry of Health, Konya Numune Hospital, 42060 Konya, Turkey
[4]Department of Medical Services and Techniques, Istanbul Rumeli University, Vocational School of Health Services, 34570 Istanbul, Turkey
[5]Department of Pathology, Kastamonu University School of Medicine, 37200 Kastamonu, Turkey
[6]Department of Medical Biochemistry, Kastamonu University School of Medicine, 37200 Kastamonu, Turkey
[7]Department of Surgery, Faculty of Veterinary, Kastamonu University, 37200 Kastamonu, Turkey

Received: 3 August 2025 / Accepted: 10 September 2025
Published online: 08 October 2025

References

1. Gill TK, et al. Global, regional, and national burden of other musculoskeletal disorders, 1990–2020, and projections to 2050: a systematic analysis of the Global Burden of Disease Study 2021. Lancet Rheumatol. 2023;5:e670–82. https://doi.org/10.1016/S2665-9913(23)00232-1.
2. Nicholson JA, Makaram N, Simpson A, Keating JF. Fracture nonunion in long bones: a literature review of risk factors and surgical management. Injury. 2021;52(Suppl 2):S3–11.
3. Liu C, Carrera R, Flamini V, Kenny L, Cabahug-Zuckerman P, George BM, et al. Effects of mechanical loading on cortical defect repair using a novel mechanobiological model of bone healing. Bone. 2018;108:145–55.
4. Behrends DA, Hui D, Gao C, Awlia A, Al-Saran Y, Li A, et al. Defective bone repair in c57bl6 mice with acute systemic inflammation. Clin Orthop Relat Res. 2017;475:906–16.
5. Foster NE, Pincus T, Underwood MR, Vogel S, Breen A, Harding G. Understanding the process of care for musculoskeletal conditions—Why a biomedical approach is inadequate. Rheumatology. 2003;42:401–4.
6. Al-Worafi YM. Musculoskeletal diseases: causes and risk factors in developing countries. In: Al-Worafi YM, editor. Handbook of medical and health sciences in developing countries. Cham: Springer; 2024. p. 1–21.
7. Lin I, Wiles L, Waller R, Goucke R, Nagree Y, Gibberd M, et al. What does best practice care for musculoskeletal pain look like? Eleven consistent recommendations from high-quality clinical practice guidelines: systematic review. Br J Sports Med. 2020;54:79–86. https://doi.org/10.1136/bjsports-2018-099878.
8. Connelly LB, Woolf A, Brooks P. Cost-effectiveness of interventions for musculoskeletal conditions. In: Jamison DT, Breman JG, Measham AR, et al., editors. Disease control priorities in developing countries. 2nd ed. Washington DC: The International Bank for Reconstruction and Development/The World Bank; 2006. Chapter 51. Available from: https://www.ncbi.nlm.nih.gov/books/NBK11713/. Co-published by Oxford University Press, New York.
9. Varela-Eirin M, Loureiro J, Fonseca E, Corrochano S, Caeiro JR, Collado M, et al. Cartilage regeneration and aging: targeting cellular plasticity in osteoarthritis. Ageing Res Rev. 2018;42:56–71. https://doi.org/10.1016/j.arr.2017.12.006.
10. Khajuria DK, Karuppagounder V, Nowak I, Sepulveda DE, Lewis GS, Norbury CC, et al. Cannabidiol and cannabigerol, nonpsychotropic cannabinoids, as analgesics that effectively manage bone fracture pain and promote healing in mice. J Bone Miner Res. 2023;38:1560–76. https://doi.org/10.1002/jbmr.4902.
11. Kogan NM, Melamed E, Wasserman E, Raphael B, Breuer A, Stok KS, et al. Cannabidiol, a major non-psychotropic cannabis constituent enhances fracture healing and stimulates lysyl hydroxylase activity in osteoblasts. J Bone Miner Res. 2015;30:1905–13. https://doi.org/10.1002/jbmr.2513.
12. Zhou W, Huang W, Shen X, Huang K, Tian R, Yuan Y, et al. Activation of GLP-1 receptors enhances the osteogenic differentiation process of STRO-1-positive BMSCs. Mol Biol Rep. 2025;52:559. https://doi.org/10.1007/s11033-025-10648-3.
13. Meng J, Ma X, Wang N, Jia M, Bi L, Wang Y, et al. Activation of GLP-1 receptor promotes bone marrow stromal cell osteogenic differentiation through β-catenin. Stem Cell Rep. 2016;6:579–91. https://doi.org/10.1016/j.stemcr.2016.02.002.
14. Zhai S, Liu C, Vimalraj S, Subramanian R, Abullais SS, Arora S, et al. Glucagon-like peptide-1 receptor promotes osteoblast differentiation of dental pulp stem cells and bone formation in a zebrafish scale regeneration model. Peptides. 2023;163:170974. https://doi.org/10.1016/j.peptides.2023.170974.
15. Hulsart-Billström G, Bergman K, Andersson B, Hilborn J, Larsson S, Jonsson KB. A uni-cortical femoral defect model in the rat: evaluation using injectable hyaluronan hydrogel as a carrier for bone morphogenetic protein-2. J Tissue Eng Regen Med. 2015;9:799–807. https://doi.org/10.1002/term.1655.
16. Taleb OMA, Wissa MY, Nour RKAE, Awad HA, Moussa NM. Potential effectiveness of exenatide in experimentally-induced osteoporosis. Egypt Rheumatol. 2020;42:57–62. https://doi.org/10.1016/j.ejr.2019.06.003.
17. Einhorn TA, Gerstenfeld LC. Fracture healing: mechanisms and interventions. Nat Rev Rheumatol. 2015;11:45–54.
18. Lutz C, Recknagel S, Ignatius A. Fracture healing under healthy and inflammatory conditions. Nat Rev Rheumatol. 2012;8:133–43.
19. Kon T, Cho TJ, Aizawa T, Yamazaki M, Nooh N, Graves D, et al. Expression of osteoprotegerin, receptor activator of NF-kappaB ligand (osteoprotegerin ligand) and related proinflammatory cytokines during fracture healing. J Bone Miner Res. 2001;16:1004–14. https://doi.org/10.1359/jbmr.2001.16.6.1004.
20. Huo MH, Troiano NW, Pelker RR, Gundberg CM, Friedlaender GE. The influence of ibuprofen on fracture repair: Biomechanical, biochemical, histologic, and histomorphometric parameters in rats. J Orthop Res. 1991;9:383–90. https://doi.org/10.1002/jor.1100090310.
21. Deganutti G, Liang YL, Zhang X, Khoshouei M, Clydesdale L, Belousoff MJ, et al. Dynamics of GLP-1R peptide agonist engagement are correlated with kinetics of G protein activation. Nat Commun. 2022;13:92. https://doi.org/10.1038/s41467-021-27760-0.
22. Naismith JH, Devine TQ, Kohno T, Sprang SR. Structures of the extracellular domain of the type I tumor necrosis factor receptor. Structure. 1996;4:1251–62. https://doi.org/10.1016/s0969-2126(96)00134-7.
23. Boulanger MJ, Chow DC, Brevnova EE, Garcia KC. Hexameric structure and assembly of the interleukin-6/IL-6 alpha-receptor/gp130 complex. Science. 2003;300:2101–4. https://doi.org/10.1126/science.1083901.
24. Migliorini F, Pilone M, Eschweiler J, El Mansy Y, Maffulli N, Schenker H. Pharmacological interventions for fracture healing: a systematic review of randomized controlled trials. Injury. 2023;54:3673–82. https://doi.org/10.1016/j.injury.2023.08.052.
25. Martinez de Albornoz P, Khanna A, Longo UG, Forriol F, Maffulli N. The evidence of low-intensity pulsed ultrasound for in vitro, animal and human fracture healing. Br Med Bull. 2011;100:39–57. https://doi.org/10.1093/bmb/ldr003.
26. Berni M, Brancato AM, Torriani C, Bina V, Annunziata S, Cornella E, et al. The role of low-level laser therapy in bone healing: systematic review. Int J Mol Sci. 2023;24:7094. https://doi.org/10.3390/ijms24087094.
27. Caliogna L, Medetti M, Bina V, Brancato AM, Castelli A, Jannelli E, et al. Pulsed electromagnetic fields in bone healing: molecular pathways and clinical applications. Int J Mol Sci. 2021;22:7403. https://doi.org/10.3390/ijms22147403.
28. Niikura T, Sakai Y, Lee SY, Oe K, Iwakura T, Kurosaka M. Intermittent pneumatic compression for treating bone and soft-tissue healing: a systematic review. J Bone Jt Surg Am. 2008;90:1689–96. https://doi.org/10.2106/JBJS.G.00686.
29. Ji X, Zhao D, Xin Z, Feng H, Huang Z. The predictive value of stress-induced hyperglycemia parameters for delayed healing after tibial fracture post-surgery. J Orthop Surg Res. 2024;19:666. https://doi.org/10.1186/s13018-024-05138-4.
30. Liu J, Liu TT, Zhang HC, Li C, Wei W, Chao AJ. Effects of Jintiange on the healing of osteoporotic fractures in aged rats. J Orthop Surg Res. 2024;19:828. https://doi.org/10.1186/s13018-024-05351-1.
31. Zhang Z, Wang L, Zhang F, Jing S, Cen M. Functional mechanism and clinical implications of mir-1271-5p in pilon fracture healing processes. J Orthop Surg Res. 2024;19:782. https://doi.org/10.1186/s13018-024-05291-w.
32. Wu X, Shen T, Ji W, Huang M, Sima J, Li J, et al. LncRNA CASC11 regulates the progress of delayed fracture healing via sponging miR-150-3p. J Orthop Surg Res. 2024;19:757. https://doi.org/10.1186/s13018-024-05226-5.
33. Li Y, Sun Y, Ma K, Wang S, Wang Z, Huang L. Functional mechanism and clinical implications of LINC00339 in delayed fracture healing. J Orthop Surg Res. 2024;19:511. https://doi.org/10.1186/s13018-024-04998-0.
34. Ma X, Meng J, Jia M, Bi L, Zhou Y, Wang Y, et al. Exendin-4, a glucagon-like peptide-1 receptor agonist, prevents osteopenia by promoting bone formation and suppressing bone resorption in aged ovariectomized rats. J Bone Miner Res. 2013;28:1641–52. https://doi.org/10.1002/jbmr.1898.
35. Pereira M, Jeyabalan J, Jørgensen CS, Hopkinson M, Al-Jazzar A, Roux JP, et al. Chronic administration of glucagon-like peptide-1 receptor agonists

improves trabecular bone mass and architecture in ovariectomised mice. Bone. 2015;81:459–67. https://doi.org/10.1016/j.bone.2015.08.006.
36. Sun HX, Lu N, Liu DM, Zhao L, Sun LH, Zhao HY, et al. The bone-preserving effects of exendin-4 in ovariectomized rats. Endocrine. 2016;51:323–32. https://doi.org/10.1007/s12020-015-0667-x.
37. Pereira M, Gohin S, Roux JP, Fisher A, Cleasby ME, Mabilleau G, et al. Exenatide improves bone quality in a murine model of genetically inherited type 2 diabetes mellitus. Front Endocrinol. 2017;8:327. https://doi.org/10.3389/fendo.2017.00327.
38. Mabilleau G, Mieczkowska A, Chappard D. Use of glucagon-like peptide-1 receptor agonists and bone fractures: a meta-analysis of randomized clinical trials. J Diabetes. 2014;6:260–6. https://doi.org/10.1111/1753-0407.12102.
39. Eminov E, Hortu I, Akman L, Erbas O, Yavasoglu A, Cirpan T. Exenatide preserves trabecular bone microarchitecture in experimental ovariectomized rat model. Arch Gynecol Obstet. 2018;297:1587–93. https://doi.org/10.1007/s00404-018-4776-7.
40. Mansur SA, Mieczkowska A, Flatt PR, Chappard D, Irwin N, Mabilleau G. The GLP-1 receptor agonist exenatide ameliorates bone composition and tissue material properties in high fat fed diabetic mice. Front Endocrinol. 2019;10:51. https://doi.org/10.3389/fendo.2019.00051.
41. Cai TT, Li HQ, Jiang LL, Wang HY, Luo MH, Su XF, et al. Effects of GLP-1 receptor agonists on bone mineral density in patients with type 2 diabetes mellitus: a 52-week clinical study. BioMed Res Int. 2021. https://doi.org/10.1155/2021/3361309.
42. Maddaloni E, Coleman RL, Holman RR. Risk factors for bone fractures in type 2 diabetes and the impact of once-weekly exenatide: insights from an EXSCEL post-hoc analysis. Diabetes Res Clin Pract. 2025;223:112125. https://doi.org/10.1016/j.diabres.2025.112125.
43. Akyay OZ, Canturk Z, Selek A, Cetinarslan B, Tarkun İ, Cakmak Y, et al. The effects of exenatide and insulin glargine treatments on bone turnover markers and bone mineral density in postmenopausal patients with type 2 diabetes mellitus. Medicine. 2023;102:e35394. https://doi.org/10.1097/MD.0000000000035394.
44. Xiao Y, Zhou M, Xiao W. Fracture events associated with GLP-1 receptor agonists in FDA adverse events reporting system. Acta Diabetol. 2025;62:1009–10021. https://doi.org/10.1007/s00592-024-02415-w.
45. Su B, Sheng H, Zhang M, Bu L, Yang P, Li L, et al. Risk of bone fractures associated with glucagon-like peptide-1 receptor agonists' treatment: a meta-analysis of randomized controlled trials. Endocrine. 2015;48:107–15. https://doi.org/10.1007/s12020-014-0361-4.
46. Zhao C, Liang J, Yang Y, Yu M, Qu X. The impact of glucagon-like peptide-1 on bone metabolism and its possible mechanisms. Front Endocrinol. 2017;8:98. https://doi.org/10.3389/fendo.2017.00098.
47. Wang M, Li Y, Sui F. Letter to "Risk factors for bone fractures in type 2 diabetes and the impact of once-weekly exenatide: Insights from an EXSCEL post-hoc analysis." Diabetes Res Clin Pract. 2025;224:112199. https://doi.org/10.1016/j.diabres.2025.112199.
48. Hussein AI, Mancini C, Lybrand KE, Cooke ME, Matheny HE, Hogue BL, et al. Serum proteomic assessment of the progression of fracture healing. J Orthop Res. 2018;36:1153–63. https://doi.org/10.1002/jor.23754.
49. Zheng XQ, Huang J, Lin JL, Song CL. Pathophysiological mechanism of acute bone loss after fracture. J Adv Res. 2023;49:63–80. https://doi.org/10.1016/j.jare.2022.08.019.
50. Fischer V, Haffner-Luntzer M, Prystaz K, Vom Scheidt A, Busse B, Schinke T, et al. Calcium and vitamin D deficiency marginally impairs fracture healing but aggravates posttraumatic bone loss in osteoporotic mice. Sci Rep. 2017;7(1):7223. https://doi.org/10.1038/s41598-017-07511-2.
51. Ciosek Ż, Kot K, Kosik-Bogacka D, Łanocha-Arendarczyk N, Rotter I. The effects of calcium, magnesium, phosphorus, fluoride, and lead on bone tissue. Biomolecules. 2021;11:506. https://doi.org/10.3390/biom11040506.
52. Sabokbar A, Millett PJ, Myer B, Rushton N. A rapid, quantitative assay for measuring alkaline phosphatase activity in osteoblastic cells in vitro. Bone Miner. 1994;27:57–67. https://doi.org/10.1016/s0169-6009(08)80187-0.
53. Taniguchi T, Tomoko M, Shindo H. Changes of serum levels of osteocalcin, alkaline phosphatase, IGF-I and IGF-binding protein-3 during fracture healing. Injury. 2003;34:477–9.
54. Shu J, Tan A, Li Y, Huang H, Yang J. The correlation between serum total alkaline phosphatase and bone mineral density in young adults. BMC Musculoskelet Disord. 2022;23:467. https://doi.org/10.1186/s12891-022-05438-y.
55. Chen Z, Xie L, Xu J, Lin X, Ye J, Shao R, et al. Changes in alkaline phosphatase, calcium, C-reactive protein, D-dimer, phosphorus, and hemoglobin in elderly osteoporotic hip fracture patients. Ann Palliat Med. 2021;10:1079–88. https://doi.org/10.21037/apm-20-218.
56. Kitaura H, Marahleh A, Ohori F, Noguchi T, Nara Y, Pramusita A, et al. Role of the interaction of tumor necrosis factor-α and tumor necrosis factor receptors 1 and 2 in bone-related cells. Int J Mol Sci. 2022;23:1481. https://doi.org/10.3390/ijms23031481.
57. Zhao W, Li J, Su T, Wang C, Fu Y, Li C, et al. Osteoclast activation and inflammatory bone diseases: focusing on receptors in osteoclasts. J Inflamm Res. 2025;18:3201–13. https://doi.org/10.2147/JIR.S507269.
58. Mountziaris PM, Tzouanas SN, Mikos AG. The interplay of bone-like extracellular matrix and TNF-α signaling on in vitro osteogenic differentiation of mesenchymal stem cells. J Biomed Mater Res A. 2012;100:1097–106. https://doi.org/10.1002/jbm.a.34058.
59. Luo G, Li F, Li X, Wang ZG, Zhang B. TNF α and RANKL promote osteoclastogenesis by upregulating RANK via the NF κB pathway. Mol Med Rep. 2018;17:6605–11. https://doi.org/10.3892/mmr.2018.8698.
60. Fischer V, Küppers O, Steppe L, Krüger BT, Hidalgo J, Haffner-Luntzer M, et al. Physiological fracture healing is unaffected by neutrophil-derived IL-6 or IL-6R signaling in mice. Shock. 2025. https://doi.org/10.1097/SHK.0000000000002615.
61. Kaiser K, Prystaz K, Vikman A, Haffner-Luntzer M, Bergdolt S, Strauss G, et al. Pharmacological inhibition of IL-6 trans-signaling improves compromised fracture healing after severe trauma. Naunyn Schmiedebergs Arch Pharmacol. 2018;391:523–36. https://doi.org/10.1007/s00210-018-1483-7.
62. Pesic G, Jeremic J, Nikolic T, Zivkovic V, Srejovic I, Vranic A, et al. Interleukin-6 as possible early marker of stress response after femoral fracture. Mol Cell Biochem. 2017;430:191–9. https://doi.org/10.1007/s11010-017-2967-3.
63. Moriishi T, Ozasa R, Ishimoto T, Nakano T, Hasegawa T, Miyazaki T, et al. Osteocalcin is necessary for the alignment of apatite crystallites, but not glucose metabolism, testosterone synthesis, or muscle mass. PLoS Genet. 2020;16:e1008586. https://doi.org/10.1371/journal.pgen.1008586.
64. Manolagas SC. Osteocalcin promotes bone mineralization but is not a hormone. PLoS Genet. 2020;16:e1008714. https://doi.org/10.1371/journal.pgen.1008714.
65. Martiniakova M, Biro R, Kovacova V, Babikova M, Zemanova N, Mondockova V, et al. Current knowledge of bone-derived factor osteocalcin: its role in the management and treatment of diabetes mellitus, osteoporosis, osteopetrosis, and inflammatory joint diseases. J Mol Med. 2024;102:435–52. https://doi.org/10.1007/s00109-024-02418-8.
66. Chatzipetros E, Damaskos S, Tosios KI, Christopoulos P, Donta C, Kalogirou EM, et al. The effect of nano-hydroxyapatite/chitosan scaffolds on rat calvarial defects for bone regeneration. Int J Implant Dent. 2021;7(1):40. https://doi.org/10.1186/s40729-021-00327-w.
67. Yilmaz I, Karaarslan N. Examining the effects of HMG-CoA reductase inhibitors on anabolic and catabolic signaling pathway proteins associated with degenerative disc disease. Eur Rev Med Pharmacol Sci. 2022;26:2990–3000. https://doi.org/10.26355/eurrev_202204_28630.
68. Yilmaz I, Akalan H, Oznam K, Karaarslan N, Yasar Sirin D, Ozbek H. Does oseltamivir protect human chondrocyte and nucleus pulposus cells from degeneration by inhibiting senescence and proinflammation mediated by the NLRP3 inflammasome and NF-κB? Eur Rev Med Pharmacol Sci. 2022;26:4816–27. https://doi.org/10.26355/eurrev_202207_29207.
69. Yilmaz I, Karaarslan N, Ozbek H. Practical performance of hippocampal tissue resection in rats in pharmacomolecular research. Turk Neurosurg. 2021;31:112–8.

Publisher's note